

## Solving the Cauchy Problem of the Nonlinear Steady-state Heat Equation Using Double Iteration Process

Weichung Yeih<sup>1,2</sup>, I-Yao Chan<sup>1</sup>, Chia-Ming Fan<sup>1</sup>, Jiang-Jhy Chang<sup>1</sup> and Chein-Shan Liu<sup>3</sup>

**Abstract:** In this paper, the Cauchy inverse problem of the nonlinear steady-state heat equation is studied. The double iteration process is used to tackle this problem in which the outer loop is developed based on the residual norm based algorithm (RNBA) while the inner loop determines the evolution direction and the modified Tikhonov's regularization method (MTRM) developed by Liu (Liu, 2012) is adopted. For the conventional iteration processes, a fixed evolution direction such as  $\mathbf{F}$ ,  $\mathbf{B}^{-1}\mathbf{F}$ ,  $\mathbf{B}^T\mathbf{F}$  or  $\alpha\mathbf{F}+(1-\alpha)\mathbf{B}^T\mathbf{F}$  is used where  $\mathbf{F}$  is the residual vector,  $\mathbf{B}$  is the Jacobian matrix, the superscript '-1' denotes the inverse, the superscript 'T' denotes the transpose of a matrix and  $\alpha$  denotes the optimal coefficient. Unlike the conventional approaches, the current approach tries to find an appropriate direction from the initial guess  $\mathbf{B}^T\mathbf{F}$  using the MTRM and the final evolution direction is determined once the value of  $a_0$  is less than the critical value  $a_c$ . Since it may consume too much computation time for searching this appropriate evolution direction such that it makes this process computationally noneconomic, we terminate the inner iteration process as well as the whole process once the number of the iteration steps for the inner iteration exceeds a given maximum value, says  $I_{max}$ . Six examples are illustrated to show the validity of the current approach and results show that the proposed method is very efficient and accurate.

**Keywords:** Cauchy problem, steady-state, modified Tikhonov's regularization method.

### 1 Introduction

In this paper, the nonlinear steady-state heat equation is studied. The nonlinearity occurs from the fact that the heat conduction coefficient is temperature-dependent.

<sup>1</sup> Department of Harbor and River Engineering & Computation and Simulation Center, National Taiwan Ocean University, 202 Keelung, Taiwan, ROC.

<sup>2</sup> Corresponding author. e-mail: wcyeih@mail.ntou.edu.tw

<sup>3</sup> Department of Civil Engineering, National Taiwan University, Taipei, 106-17 Taiwan.

There are many applications for this kind of materials. For example, the nanofluid [Mintsa, Roy, Nguyen and Doucet (2009)], single-walled carbon nanotubes [Hone, Whitney, Piskoti and A. Zettl (1999)] and porous silicon [Gesele, Linsmeier, Drach, Fricke and Arens-Fischer (1997)] have been used and they all have temperature-dependent conductivity. To deal with the problems for this kind of materials numerically, one can use the Kirchhoff transformation to convert the nonlinear governing equation into a linear one [Bialecki and Nowak (1981)]. In the existing literatures, most researchers focused on the standard boundary value problem. Only limited literatures deal with the inverse problems. Cannon (1967) studied the steady-state heat equation subject to the boundary condition: Neumann boundary condition on the whole boundary and Dirichlet boundary condition on part of the boundary. Ingham and Yuan (1993) solved the inverse problem of determining the unknown temperature-dependent thermal conductivity and temperature distribution by prescribing the temperature boundary condition on the whole boundary and several interior points. To authors' best knowledge, the inverse Cauchy problem (seeking the temperature distribution subject to the Dirichlet data and Neumann data on part of the boundary and no information on the remaining) for this nonlinear elliptic type equation has rarely been investigated. In the following, we will give a brief review for the development of solvers of nonlinear algebraic equations especially for ill-posed system.

Nonlinear problems are often encountered in science and engineering. Many phenomena are modeled as nonlinear equations. For numerical calculations, after discretization a set of nonlinear algebraic equation is constructed. To solve nonlinear algebraic equations, there exist many well-developed methods. The most well known method is the so-called Newton-Raphson method [Tjalling (1955)] (also known as the Newton method) where the iteration process is written as:

$$\mathbf{x}_{k+1} = \mathbf{x}_k + \mathbf{B}_k^{-1} \mathbf{F}_k \quad (1)$$

where  $\mathbf{x}$  denotes the unknown vector. It is known that the Newton-Raphson method converges very fast. However, when the system is large the inverse of the Jacobian matrix will become impossible. In addition, if the Jacobian matrix is very ill-conditioned it is non-trivial to have accurate estimate for its inverse. This may result in numerical instability for the Newton's method. It means that for the inverse problems which are known for their ill-posedness using the Newton's method will yield inaccurate answers.

Therefore, for nonlinear ill-posed problems other alternatives are suggested. In the Landweber [Landweber (1951)] iteration method, the direction of  $\mathbf{B}^T \mathbf{F}$  is used and the iteration is written as:

$$\mathbf{x}_{k+1} = \mathbf{x}_k + \mathbf{B}_k^T \mathbf{F}_k. \quad (2)$$

However, the Landweber iteration method may not overcome the ill-posed behaviors for some systems and the Tikhonov's regularization method [Tikhonov & Arsenin (1977)] is usually adopted. However, for conventional Tikhonov's regularization method, to determine the optimal regularization parameter requires a lot of computation efforts such as the L-curve method [Hanson (1992)] or the discrepancy principles [Morozov (1984, 1966)]. An easier method to determine the regularization method has been proposed by Liu and Kuo (2011).

Other alternatives to tackle the ill-posed problems are derived from the evolution dynamics. For example, the fictitious time integration method (FTIM) was proposed by Liu and Atluri (2008) where the direction  $\mathbf{F}$  is chosen. Similarly, the dynamic Jacobian inverse free method (DJIFM) proposed by Ku, Yeih and Liu (2011) has adopted the direction  $\mathbf{F}$  multiplying with a modification factor to ensure that the trajectory of the unknown vector lies on the manifold. The exponentially convergent scalar homotopy method (ECSHA) adopts the direction of  $\mathbf{B}^T \mathbf{F}$  which is very similar to the Landweber iteration method. However, ECSHA multiplies the direction of evolution by a modification factor which ensures that the trajectory of the unknown vector lies on the manifold. Several literatures using ECSHA to deal with ill-posed problems can be found, such as Chan and Fan (2013) and Chan, Fan and Yeih (2011). Liu and Atluri (2011a) proposed to use a direction mixed by  $\mathbf{F}$  and  $\mathbf{B}^T \mathbf{F}$ . Following this work, Yeih, Ku, Liu and Chan (2013) found the optimal direction mixed by many known directions.

However, all the above-mentioned methods adopt a specific known direction. From numerical experience, selecting a specific direction will encounter slow convergence for some cases. Recently, Yeih, Chan, Ku, Fan and Guan (2014) has proposed a double iteration process to tackle the ill-posed problem in which for each step the direction of evolution is determined from an inner iteration process and this direction does not keep a same format such as  $\mathbf{F}$  or  $\mathbf{B}^T \mathbf{F}$ . Theoretically speaking, this method tries to find a direction as close  $\mathbf{B}^{-1} \mathbf{F}$  as possible and avoid numerical instability at the same time.

In this paper, we investigate the nonlinear ill-posed inverse problem: the Cauchy inverse problem of the nonlinear steady-state heat equation. The double iteration process will be used. Aside from this section, the following sections will be arranged. In Section 2, mathematical backgrounds will be given. In Section 3, six numerical examples will be illustrated to show the validity of this method. In the final section, a brief conclusion will be given based on the findings in previous sections.

**2 Mathematical backgrounds**

**2.1 Problem formulation**

The nonlinear steady-state heat equation for a 2D compact region is written as:

$$\nabla \cdot (k(T) \nabla T) = \frac{\partial}{\partial x} \left( k \frac{\partial T}{\partial x} \right) + \frac{\partial}{\partial y} \left( k \frac{\partial T}{\partial y} \right) = 0 \tag{3}$$

where  $k$  is the temperature-dependent heat conduction coefficient and  $T$  is the temperature. There are several kinds of boundary conditions:

$$T = \bar{T} \quad \text{on} \quad \Gamma_1 \quad (\text{Dirichlet boundary condition}) \tag{4}$$

$$q \equiv k \frac{\partial T}{\partial n} = \bar{q} \quad \text{on} \quad \Gamma_2 \quad (\text{Neumann boundary condition}) \tag{5}$$

$$q = k \frac{\partial T}{\partial n} = h(T_f - T) - \sigma \bar{\epsilon} (T^4 - T_s^4) \quad \text{on} \quad \Gamma_3 \quad (\text{Robin boundary condition}) \tag{6}$$

where  $q$  is the heat flux,  $n$  denotes the outward normal direction on the boundary,  $\sigma$  is the Stefan-Boltzmann constant,  $T_f$  is the temperature of the surrounding medium,  $\bar{\epsilon}$  is the temperature-dependent emissivity between the surface  $\Gamma_3$  and radiating medium at temperature  $T_s$ ,  $h$  is a constant and  $(\bar{\bullet})$  quantities indicate prescribed boundary values.  $\Gamma_i$  denotes part of the boundary. For a standard boundary value problem, for each point on the boundary only one kind of boundary condition can be given and boundary condition should be given on the whole boundary. It is well known that the standard boundary value problem is well-posed mathematically.

The inverse Cauchy problem is somewhat different from the standard boundary value problem. Overprescribed Cauchy data are given on part of the boundary, for example Dirichlet and Neumann boundary conditions or Dirichlet and Robin boundary conditions are both given on part of the boundary. Meanwhile, on the remaining part of boundary no information is given. Inverse Cauchy problems are known as an ill-posed system. To solve this ill-posed system numerically, a robust and sound solver is necessary to overcome the numerical instability.

It is worth to mention here that by using a new variable

$$\psi \equiv \int_{T_0}^T k(T) dT, \tag{7}$$

Eq.(3) will be transformed into a Laplace equation while the boundary conditions in eqs.(4)-(5) are still linear with respect to the variable  $\psi$  and Eq.(6) will become nonlinear. This technique is known as the Kirchhoff transformation. After solving

the boundary value problems of the new variable  $\psi$ , the inverse Kirchhoff transformation is then adopted to obtain the solution for the physical quantity  $T$ . In this paper, we do not adopt the Kirchhoff transformation technique and keep the original partial differential equation system nonlinear.

**2.2 Multiquadric radial basis functions**

Assume the physical quantity we concern can be expressed by the radial basis functions as:

$$T(\mathbf{x}_i) = \sum_{j=1}^m \phi_{ij}(\bar{r}(\mathbf{x}_i, \mathbf{s}_j))c_j, \tag{8}$$

where  $\mathbf{x}_i$  is the position vector of  $i$ -th observation point,  $\mathbf{s}_j$  is the position vector of the  $j$ -th source point,  $\bar{r}$  is the radial distance between  $\mathbf{x}_i$  and  $\mathbf{s}_j$ , and  $c_j$  is the undetermined coefficient.  $\phi$  is the radial basis function and in this paper the multiquadric radial basis function is selected as:

$$\phi_{ij}(\bar{r}(\mathbf{x}_i, \mathbf{s}_j)) \equiv \sqrt{\|\mathbf{x}_i - \mathbf{s}_j\|^2 + c^2} \tag{9}$$

in which  $c$  is a shape parameter and the value of  $c$  is 1.5 throughout this paper. The value of  $c$  influences the results of inverse Cauchy problems. However, if the value of  $c$  is appropriate, the influence is not significant as mentioned later in example 1. The optimal selection of  $c$  is not within the scope of this article and is left as an open problem.

More details of the multiquadric radial basis function can refer to [Hardy (1990)]. Substituting the expression in eq.(8) into eq.(3) to eq.(6) for the inverse Cauchy problem, we will construct a system of nonlinear algebraic equations for unknown coefficient  $c_j$ . Unfortunately this nonlinear algebraic equation system is ill-posed such that conventional numerical solvers fail due to the numerical instability. One can easily observe that the leading matrix for the radial basis functions is a full matrix which usually makes the ill-posed nature worse.

**2.3 Residual norm based algorithm**

The following derivation can be found in many related articles such as [Liu and Atluri (2012); Liu and Atluri (2011b)]. Let us begin with a nonlinear algebraic system written as:

$$\mathbf{F}(\mathbf{x}) = \mathbf{0}. \tag{10}$$

To solve this nonlinear algebraic equation system, an equivalent scalar equation can be written as

$$\|\mathbf{F}(\mathbf{x})\|^2 = 0. \tag{11}$$

Let us construct a space-time manifold as:

$$h(\mathbf{x},t) = \frac{1}{2} \|\mathbf{F}(\mathbf{x})\|^2 - \frac{1}{2} \frac{1}{Q(t)} \|\mathbf{F}(\mathbf{x}_0)\|^2 = 0 \tag{12}$$

where  $\mathbf{x}_0$  is the initial guess and  $Q(t)$  satisfies that  $Q(t) > 0$ ,  $Q(0) = 1$ , and it is a monotonically increasing function of  $t$  with  $Q(\infty) = \infty$ .

In order to keep the trajectory of the solution  $\mathbf{x}$  on the manifold, the following consistency equation should be satisfied:

$$\frac{Dh}{Dt} = \frac{\partial h}{\partial t} + \nabla h \cdot \frac{d\mathbf{x}}{dt} = 0. \tag{13}$$

Since equation (13) is a scalar equation, it is impossible to determine the evolution of the unknown vector (i.e.,  $\frac{d\mathbf{x}}{dt}$ ) uniquely. Let us assume that the evolution of the unknown vector is in the direction of  $\mathbf{u}$  and we have:

$$\dot{\mathbf{x}} = \frac{d\mathbf{x}}{dt} = \lambda \mathbf{u} \tag{14}$$

where  $\lambda$  is the proportional constant. After some manipulations, the evolution equation of  $\mathbf{x}$  can be found as

$$\dot{\mathbf{x}} = -\frac{\dot{Q}(t)}{2Q(t)} \frac{\|\mathbf{F}(\mathbf{x})\|^2}{\mathbf{F}^T(\mathbf{x})\mathbf{v}} \mathbf{u} \tag{15}$$

where  $\mathbf{v}=\mathbf{B}\mathbf{u}$ . Now let us consider the evolution of the residual vector as:

$$\dot{\mathbf{F}}(\mathbf{x}(t)) = \mathbf{B}\dot{\mathbf{x}}. \tag{16}$$

Substituting equation (15) into equation (16), it follows

$$\dot{\mathbf{F}}(\mathbf{x}(t)) = \frac{-\dot{Q}(t)}{2Q(t)} \frac{\|\mathbf{F}(\mathbf{x})\|^2}{\mathbf{F}^T(\mathbf{x})\mathbf{v}} \mathbf{v}. \tag{17}$$

Using the forward Euler scheme, we can discretize equation (17) as:

$$\mathbf{F}(\mathbf{x}(t + \Delta t)) = \mathbf{F}(\mathbf{x}(t)) - \Delta t \frac{\dot{Q}(t)}{2Q(t)} \frac{\|\mathbf{F}(\mathbf{x})\|^2}{\mathbf{F}^T(\mathbf{x})\mathbf{v}} \mathbf{v}. \tag{18}$$

where  $\Delta t$  is the time increment. By defining  $\beta := \Delta t \frac{\dot{Q}(t)}{2Q(t)}$  and using equation (18), one can derive an algebraic equation for  $\beta \mathbf{g}$  as

$$a_0 \beta^2 - 2\beta + 1 - \frac{Q(t)}{Q(t + \Delta t)} = 0, \tag{19}$$

where  $a_0 = \frac{\|\mathbf{F}(\mathbf{x})\|^2 \|\mathbf{v}\|^2}{(\mathbf{F}^T(\mathbf{x})\mathbf{v})^2} = \left\{ \frac{\|\mathbf{F}(\mathbf{x})\| \|\mathbf{v}\|}{(\mathbf{F}^T(\mathbf{x})\mathbf{v})} \right\}^2 = \left( \frac{1}{\cos \theta} \right)^2$  in which  $\theta$  denotes the angle between the residual vector  $\mathbf{F}$  and the vector  $\mathbf{v}$ . From the Cauchy-Schwarz inequality, it can be easily verified that  $a_0 \geq 1$ . Now let us define  $s := \frac{Q(t)}{Q(t+\Delta t)} = \frac{\|\mathbf{F}(\mathbf{x}(t+\Delta t))\|^2}{\|\mathbf{F}(\mathbf{x}(t))\|^2}$ , and  $s$  represents the ratio between the square norm of the residual vector in the next state and the square norm of the residual vector in the current state. It is for sure that we hopes  $s \leq 1$ , such that for each state the norm of the residual vector decreases. Equation (19) now can be rewritten as  $a_0\beta^2 - 2\beta + 1 - s = 0$  and we can obtain  $\beta = \frac{1 - \sqrt{1 - (1-s)a_0}}{a_0}$  if  $1 - (1-s)a_0 \geq 0$ . For simplicity, we let  $1 - (1-s)a_0 = r^2$  ( $r$  is a relaxation parameter which will be explained later) and use the definition of  $a_0$ , one can obtain:

$$s = 1 - \frac{(1 - r^2) (\mathbf{F}^T(\mathbf{x})\mathbf{v})^2}{\|\mathbf{F}(\mathbf{x})\|^2 \|\mathbf{v}\|^2}. \tag{20}$$

Now let us use the forward Euler scheme on equation (15), we can obtain the following equation

$$\mathbf{x}(t + \Delta t) = \mathbf{x}(t) - (1 - r) \frac{\mathbf{F}^T(\mathbf{x})\mathbf{v}}{\|\mathbf{v}\|^2} \mathbf{u}. \tag{21}$$

For a selected value of  $r$ , we can rewrite equation (21) as an iteration formula [Liu and Atluri (2011b)]:

$$\mathbf{x}_{k+1} = \mathbf{x}_k - (1 - r) \frac{\mathbf{F}^T(\mathbf{x}_k)\mathbf{v}_k}{\|\mathbf{v}_k\|^2} \mathbf{u}_k. \tag{22}$$

In the above equation, the relaxation parameter is used to make the iteration stabler. In a recent published paper [Liu (2013)], Liu further found the optimal value of  $r$  needs to satisfy the following relationship to guarantee the trajectory of  $\mathbf{x}$  remain on the manifold:

$$r = \left\| 1 - \frac{a_0}{2} \right\| \tag{23}$$

Liu (2013) and Ku and Yeih (2012) all reported that the value of  $a_0$  is between 1 and 4 if we hope the trajectory of  $\mathbf{x}$  remains on the manifold. From the definition of  $a_0$ , we know that the value of  $a_0$  relates to the vector  $\mathbf{F}$  and  $\mathbf{v}$  (or equivalently  $\mathbf{u}$ ). The problem now is how to find a vector  $\mathbf{v}$  (or equivalent  $\mathbf{u}$ ) such that  $a_0$  is between 1 and 4. If such a direction is found, we then select the value of  $r$  as  $r = \left\| 1 - \frac{a_0}{2} \right\|$  in equation (22). To find an appropriate direction  $\mathbf{u}$  then becomes the key. Theoretically speaking, if  $a_0=1$  then the residual norm decreases in the

fast manner. This means that the best direction  $\mathbf{u}$  will satisfy that  $\mathbf{B}\mathbf{u} - \mathbf{F} = \mathbf{0}$  (or  $\mathbf{u} = \mathbf{B}^{-1}\mathbf{F}$  if the inverse of the Jacobian matrix exists), it means that the Newton's iteration method is the best alternative. However, for ill-posed systems to seek the inverse of the Jacobian matrix sometimes is impossible due to its numerical instability. Therefore, one requires an algorithm to find an appropriate  $\mathbf{u}$  for the nonlinear ill-posed systems. To achieve this, we give a brief review of the modified Tikhonov's regularization method (MTRM) in the following subsection.

#### 2.4 Modified Tikhonov's regularization method

The details of the following descriptions can be found in [Liu (2012)]. Considering the following linear algebraic system as:

$$\mathbf{B}\mathbf{u} = \mathbf{F}. \tag{24}$$

We use the following preconditioner written as:

$$\mathbf{P}_1 := \mathbf{B}^T + \bar{\alpha}\mathbf{B}^+, \tag{25}$$

and apply this preconditioner to equation (24) then we will obtain

$$(\mathbf{B}^T\mathbf{B} + \bar{\alpha}\mathbf{I}_n)\mathbf{u} = \mathbf{B}^T\mathbf{F} + \bar{\alpha}\mathbf{B}^+\mathbf{F} \tag{26}$$

with that  $\mathbf{B}^+\mathbf{B} = \mathbf{I}_n$ , i.e.,  $\mathbf{B}^+$  is the pseudo-inverse.

It is quite interesting to find that the regularized equation in equation (26) is very similar to that of the conventional Tikhonov's regularization method. However, in equation (26) the regularization parameter  $\bar{\alpha}$  appears in the both sides of equation while for the conventional Tikhonov's regularization method it appears only in the left-hand side.

Liu (2012) proposed that one can use equation (26) to formulate an iteration process as:

$$(\mathbf{B}^T\mathbf{B} + \bar{\alpha}\mathbf{I}_n)\mathbf{u}_{p+1} = \mathbf{B}^T\mathbf{F} + \bar{\alpha}\mathbf{u}_p \tag{27}$$

The convergence criterion of the iteration process for equation (27) can be set as:  $\|\mathbf{u}_{p+1} - \mathbf{u}_p\| \leq \zeta$  where  $\zeta$  is a preselected small tolerance. Liu also provided a theoretical proof of the convergence as the following theorem states:

[Theorem 1] For Eq. (27) with  $\bar{\alpha} > 0$  the iterative sequence  $\mathbf{u}_p$  converges to the true solution  $\mathbf{u}_{true}$  monotonically.

Although the convergence of the sequence is guaranteed, in computation reality to reach the final numerical convergence it may take too many steps such that it

becomes not economic at all. It means that if one tries to find the solution of an ill-posed linear system, a lot of computation effort will be paid for the iteration process (equation (27)) and sometimes it makes this iteration not economic at all.

This algorithm needs to be further examined while it is used to solve the best direction  $\mathbf{u}$  such that  $\mathbf{Bu}-\mathbf{F}=\mathbf{0}$ . Since for each step in the iteration process stated in equation (22) for solving the nonlinear problem, this linear algebraic equation  $\mathbf{Bu}-\mathbf{F}=\mathbf{0}$  needs to be done if one tries to find the optimal direction. However, to find the solution of this linear problem may cost too many iteration steps for iteration process equation (27). Remember that we are not really interested in finding the best direction we only want to find an appropriate  $\mathbf{u}$  such that  $a_0$  is between 1 and 4. Therefore, we can check this criterion for each step of the inner iteration (equation (27)) and terminate the inner iteration when the value of  $a_0$  is less than a prescribed critical value  $a_c$ . Of course, it may still take too many steps to let  $a_0$  being less than this prescribed critical value  $a_c$  for a severely ill-posed system. It is set that if the number of iteration steps for the inner loop exceeds a preselected maximum number  $I_{max}$ , we then stop the inner loop as well as the outer loop. It means that to find an appropriate direction of evolution using the proposed algorithm already becomes not economic and the whole process should be terminated. If the values of  $a_c$  and  $I_{max}$  are selected appropriately, the numerical results are acceptable as shown in the next section.

## 2.5 Double iteration process

Based on the abovementioned backgrounds, a double iteration process has been proposed [Yeih, Chan, Ku, Fan and Guan (2014)] and stated as the followings.

*Double Iteration Process (DIP):*

Give initial guess  $\mathbf{x}_0$

Give prescribed parameters  $\varepsilon$ ,  $\bar{a}$ .

**Outer Iteration:**

For  $k=0,1,2,\dots$  Repeat

Calculate the residual vector  $\mathbf{F}_k(\mathbf{x}_k)$  and the Jacobain matrix  $\mathbf{B}_k(\mathbf{x}_k)$

**Inner Iteration:**

From the abovementioned double iteration process, we can find that the proposed method does not really try to solve the linear algebraic equation  $\mathbf{Bu}-\mathbf{F}=\mathbf{0}$  since it is expected that for the ill-posed system it may take too many iteration steps to accomplish this for the inner iteration. In order to avoid that, once the value of  $a_0$  is

Give the initial guess of  $\mathbf{u}$  as  $\mathbf{u}_0 = \frac{\mathbf{B}_k^T \mathbf{F}_k}{\|\mathbf{B}_k^T \mathbf{F}_k\|}$ ,

For  $p=1,2,\dots, I_{\max}$

Solve  $\mathbf{u}_{p+1}$  by  $(\mathbf{B}^T \mathbf{B} + \bar{\alpha} \mathbf{I}_n) \mathbf{u}_{p+1} = \mathbf{B}^T \mathbf{F} + \bar{\alpha} \mathbf{u}_p$

Construct  $\mathbf{v}_{p+1} = \mathbf{B}_k \mathbf{u}_{p+1}$

$$(a_0)_{p+1} = \frac{\|\mathbf{F}_k(\mathbf{x})\|^2 \|\mathbf{v}_{p+1}\|^2}{(\mathbf{F}_k^T(\mathbf{x}) \mathbf{v}_p)^2}$$

(a) If  $(a_0)_{p+1} \leq a_c$ , then  $(a_0)_k = (a_0)_{p+1}$ ,  $\mathbf{u}_k = \mathbf{u}_{p+1}$ ,  $\mathbf{v}_k = \mathbf{v}_{p+1}$  and one terminates the inner iteration, otherwise continue.

(b) If  $p=I_{\max}$ , terminates the whole process.

#### End of Inner Iteration

$$\text{Calculate } r_k = \left\| 1 - \frac{(a_0)_k}{2} \right\|$$

$$\mathbf{x}_{k+1} = \mathbf{x}_k - (1-r) \frac{\mathbf{F}^T(\mathbf{x}_k) \mathbf{v}_k}{\|\mathbf{v}_k\|^2} \mathbf{u}_k$$

If  $\text{RMSE} \leq \varepsilon$  or (b) is true then the outer iteration process stops; otherwise continue.

#### End of Outer Iteration Process.

less than the prescribed value  $a_c$  we claim that the appropriate direction has been found already. Of course we need to remind ourselves that while  $a_c$  approaches to one the inner iteration takes more and more steps. We expect that it may happen that finding an appropriate direction may still requires unreasonably many steps. A criterion then is set as: when the number of iteration steps for the inner iteration exceeds that maximum value  $I_{\max}$  one can stop the whole process since it becomes not economic for further searching. The appropriate values of  $a_c$ ,  $\bar{\alpha}$  and  $I_{\max}$  influence the convergence speed a lot and how to choose them depends on experience.

According to our numerical experiences, the value of  $a_c$  is suggested to in the range from 2 to 4. Once the value of  $a_c$  is less than 2, to seek the appropriate direction in the inner loop then consumes too many iteration steps. The value of  $I_{\max}$  actually depends on the selection of  $a_c$ . If the value of  $a_c$  is between 2 and 4, the value of  $I_{\max}$  is suggested to be in the range of 30,000 to 80,000 according to our numerical experiences. The selection of  $\varepsilon$  depends on the system we want to solve. If the system is a well-posed system, the value of  $\varepsilon$  can be very small such as  $10^{-7}$ .

However, if the system is an ill-posed system the value of  $\varepsilon$  should not be very big and usually  $10^{-3}$  or  $10^{-4}$  is appropriate. It should be mentioned here that actually for an ill-posed system the value of  $\varepsilon$  can be set as a small value for DIP since this tight convergence criterion cannot be reached and the whole DIP will be terminated due to the number of the inner iteration steps exceeds the maximum value  $I_{max}$ . It means the selection of  $\varepsilon$  is not critical at all. The value of  $\bar{\alpha}$  needs to be larger than the smallest eigenvalue of  $\mathbf{B}^T \mathbf{B}$  which varies step by step. In calculation reality, a big enough value is selected. However, if  $\bar{\alpha}$  is too big the iteration process for eq.(27) becomes slow.

### 3 Numerical examples

#### 3.1 Example 1

In this example, a circular domain is considered. The radius of the circle is 1 and the center locates at (5,5). The temperature dependent conductivity  $k(T) = T$ . The exact solution is selected as  $T(x,y) = \sqrt{2xy}$ . Cauchy boundary conditions (Dirichlet and Neumann) are prescribed for the upper half circle, i.e.,  $0 \leq \bar{\theta} \leq \pi$  where  $\bar{\theta}$  denotes the angle in cylindrical coordinate measuring from the center. On the remaining boundary, no information is given. In order to know how well our proposed method can be for noisy data, two cases are studied: data without any noise and data with maximum 5% absolute relative random errors. Totally, 41 points are prescribed on the boundary and for 21 of them the Cauchy data are given. A set of 145 uniformly distributed interior points are selected to solve the system. The setup of source points used for the radial basis functions is illustrated in figure 1, the solid black dots represent source points.

After the weights of radial basis functions are obtained, a set of 313 uniformly distributed points and 41 boundary points are used to construct the temperature distribution contour. The value of  $a_c$  is 2, the value of  $\bar{\alpha}$  is 0.0001, the converge criterion  $\varepsilon=0.001$  and the maximum iteration steps for the inner loop  $I_{max}=30,000$ . The initial guesses for the unknown weights of the radial basis functions are all 0.01.

In figure 2, the root mean square errors (RMSEs) for both cases are plotted with respect to the number of iteration steps for the outer loop. It can be observed that for both cases the RMSEs are not less than the convergence criterion  $\varepsilon=0.001$  before terminations. We further check the values of  $a_0$  for both cases as shown in figure 3. One can find that for the case using data without any noise the value of  $a_0$  exceeds the critical value  $a_c =2$  after 15 steps and for the case using data with maximum 5% absolute relative random errors the value of  $a_0$  exceeds the critical value  $a_c =2$  after 7 steps. It means that for both cases, the double iteration process terminates

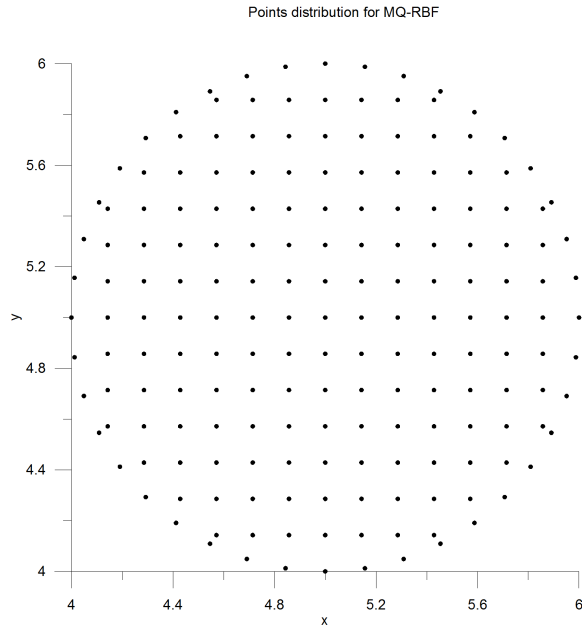


Figure 1: Distribution of source points for the radial basis functions in example 1.

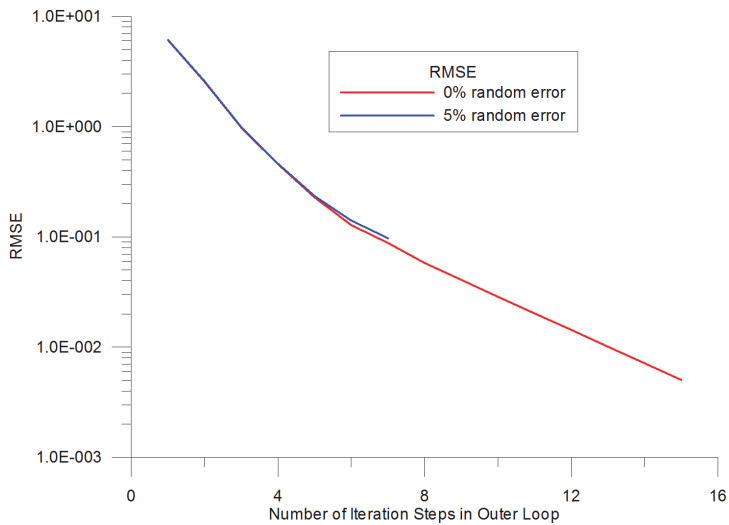


Figure 2: The root mean square errors versus the number of iteration steps for the outer loop in example 1.

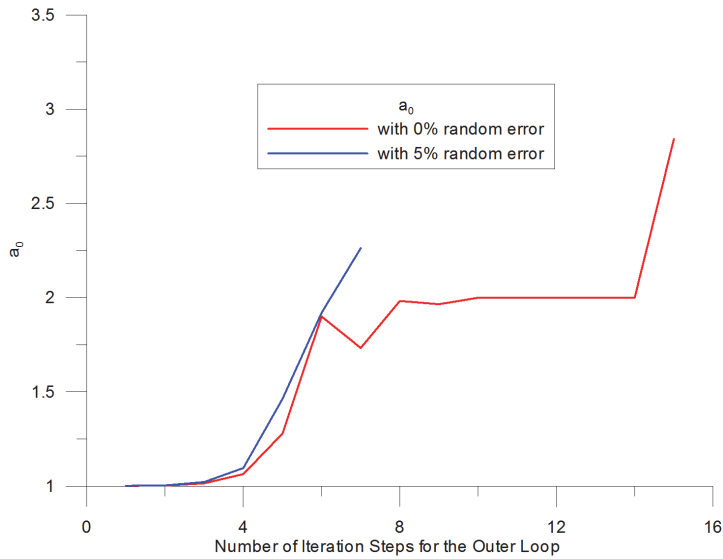


Figure 3: The profiles of  $a_0$  for both cases in example 1.

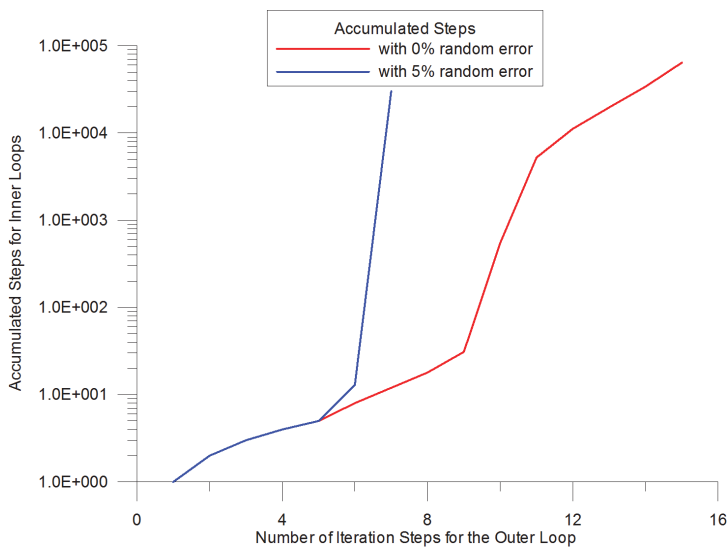


Figure 4: Profiles of accumulated steps used in the inner loops in example 1.

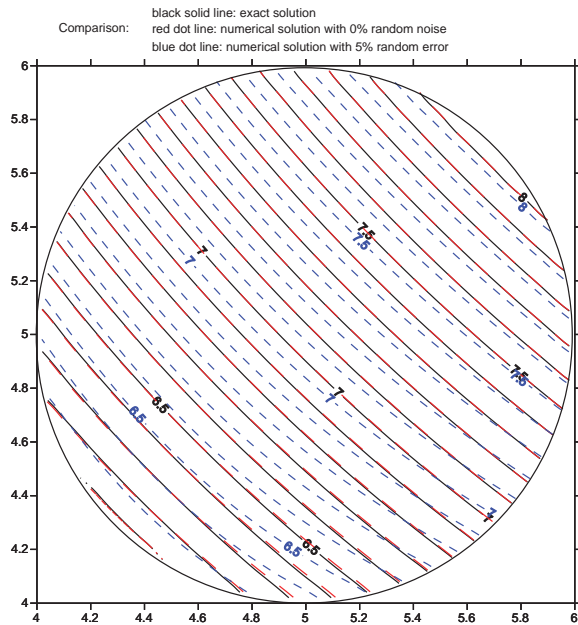


Figure 5: Comparisons between the exact solution and numerical solutions using 0% and 5% random error noise data.

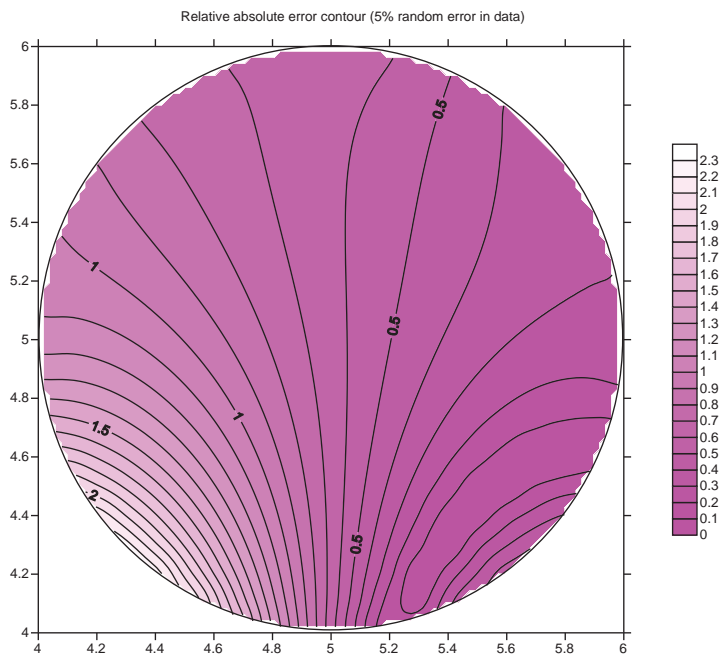


Figure 6: Relative absolute error contours for the case using 5% random error data.

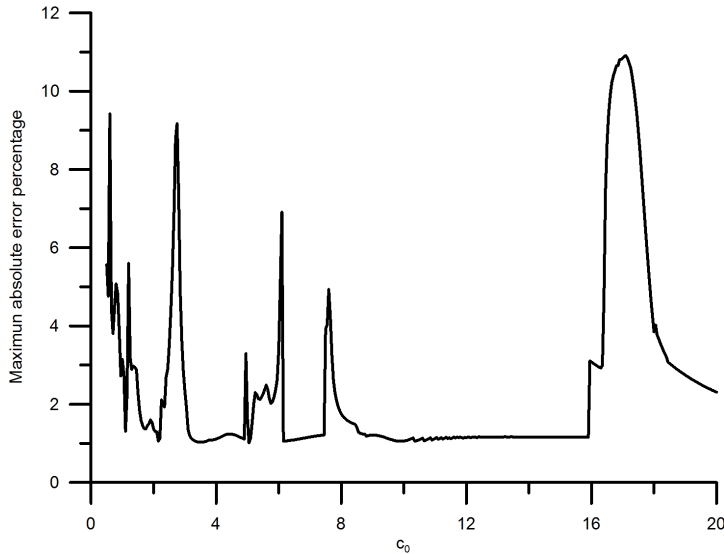


Figure 7: The maximum relative absolute error percentage for the case using 5% random error versus the shape parameter  $c$ .

because searching for the appropriate direction becomes not economic. In figure 4, we examine the total accumulate iteration steps for the inner loops for both cases. It can be found that for both cases the final accumulated steps for the inner loop are less than  $10^5$  steps. Since the most time-consuming step in the double iteration process occurs in the inner iteration loop, we can find that our proposed method indeed save computation efforts. Nevertheless, we still need to check whether or not the solution is acceptable. In figure 5, it can be seen that for the case using 0% error data the solution perfectly matches the exact solution while for the case using 5% absolute relative random error data the solution deviates from the exact solution a little bit. From figure 6, we can understand how the relative absolute error percentage distribution for the case using 5% absolute relative random error data is. It can be found the maximum absolute relative error percentage is about 2.4%. This result is quite good for the inverse Cauchy problem, especially the case we are studying now is nonlinear. Before closing this example, we use the parameters in this example and change the value of shape parameter  $c$  for the MQ radial basis functions and examine the maximum relative error for all representation points for each  $c$ . The range of  $c$  is from 0.5 to 20, and the increment in  $c$  is 0.05. The absolute relative random error up to 5% is added in Cauchy data. The result is shown in figure 7 and one can see that within this range the maximum relative error for each  $c$  is less than 12%. Actually, if the value of  $c$  is less than 0.5, the

maximum absolute relative error is very large (up to 300% or more). From this figure, one also can find that if  $c$  is in this range the influence of  $c$  is not significant. Therefore, in all cases studied in this article the value of  $c$  is set as 1.5.

### 3.2 Example 2

In this example, an annular region is considered. The outer radius for this annular region is 3 while the inner radius is 1.5. The center of this annular region is (0,0). The temperature dependent conductivity  $k(T) = T$ . The exact solution is designed as  $T(x,y) = \sqrt{2\ln(x^2+y^2)}$ . Totally 80 points are arranged on the boundary, 40 on the inner circle and 40 on the outer circle. Totally 108 uniformly distributed interior points are selected as the source points for the radial basis functions. The setup for the source points are shown in figure 8. After obtaining the weights, the temperature distribution is plotted using 228 uniformly distributed interior points and 80 boundary points.

Two Cauchy problems are investigated here: for the first problem the Cauchy data are prescribed for the outer circle and no information is prescribed for the inner circle, for the second problem the Cauchy data are prescribed for the inner circle and no information is prescribed for the outer circle. For each Cauchy problem, the numerical solutions are obtained using data without any noise and data with maximum 5% relative absolute random errors. The value of  $a_c$  is 3.5, the value of  $\bar{\alpha}$  is 0.0001, the converge criterion  $\varepsilon=0.0001$  and the maximum iteration steps for the inner loop  $I_{max}=50,000$ . The initial guesses for the unknown weights of the radial basis functions are all 0.01.

The numerical results for both cases are illustrated in figures 9 and 10, respectively. It can be found that the numerical results using data without any noise are better than that using data with maximum 5% absolute relative random errors. Basically, no much difference can be found in both cases. The accuracies for both cases are very similar. The performances of the double iteration process are tabulated in table 1. The CPU times in this table represents the performances using Pentium ® dual-core CPU E5200 at 2.50 GHz operating frequency. One can find out that due to the nonlinearity, as using data with maximum 5% absolute relative random error the maximum absolute relative error percentages are about 10% for both cases. In addition, from figures 8 and 9, one can find that the error tends to be larger near the boundary without information. Although the maximum relative error percentages for both cases are similar, it still can be told that using Cauchy data on the outer circle is better than using Cauchy data on the inner circle from the contour plots in figures 9 and 10.

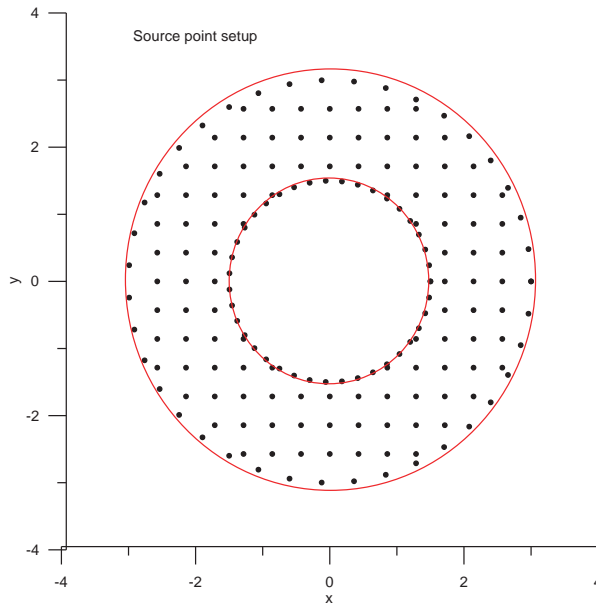


Figure 8: Source point setup for example 2.

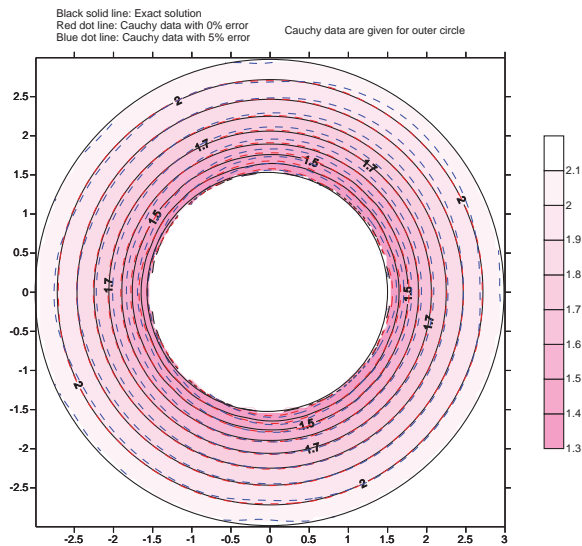


Figure 9: The temperature distribution for the Cauchy problem using data on the outer circle boundary.

Table 1 : Performance of double iteration process for example 2.

Case	Maximum error percentage in Cauchy data	CPU time (sec)	Maximum relative absolute error percentage	Total number of the iteration steps in outer loop	RMSE	Total accumulated steps for the inner loop
Cauchy data for outer circle	0	9.547	3.57	55	1.7181210e-003	56188
	5	7.984	10.7761	20	2.9552572e-002	56603
Cauchy data for inner circle	0	11.5	3.7142	61	1.4084640e-003	105342
	5	13	10.8984	23	2.2495752e-002	94633

### 3.3 Example 3

In this example, a square region defined by  $\{(x,y)|0 \leq x \leq 1; 0 \leq y \leq 1\}$  is considered. The temperature-dependent thermal conductivity is  $k(T) = \exp(T)$ . The temperature-dependent thermal conductivity now is nonlinear with respect to the temperature and it is very interesting to see what it will influence the numerical algorithm. The exact solution is designed as:  $T(x,y) = \log(xy + 5)$ . Totally 100 points (25 points for each side and points are not placed at the corners) are arranged on the boundary and 169 uniformly distributed interior points accompanied with boundary points are used to be source points. After the weights are obtained, 841 uniformly distributed interior points accompanied with boundary points are used to yield the temperature distribution. Cauchy data are given on the boundaries:  $y=0$  and  $x=0$ . Two cases are examined: Cauchy data without any noise and Cauchy data with maximum 5% random relative absolute errors. The value of  $a_c$  is 3.5, the value of  $\bar{\alpha}$  is 0.001, the converge criterion  $\varepsilon=0.0001$  and the maximum iteration steps for the inner loop  $I_{max}=50,000$ . The initial guesses for the unknown weights of the radial basis functions are all 0.01.

The numerical solutions are illustrated in figure 11. Although it looks like that the temperature contour for the solution using Cauchy data with 5% random error seems not so close to the exact solution, the maximum absolute error percentage

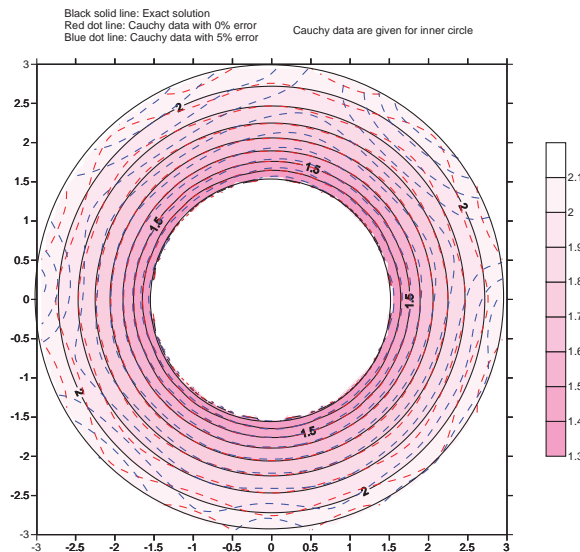


Figure 10: The temperature distribution for the Cauchy problem using data on the inner circle boundary.

for all points is only 1.4677 percent. The reason why it looks so comes from that the difference between two adjacent contour lines is 0.01 which is very small. The computational CPU time for data without error is 20.063 sec and for data with maximum 5% absolute relative random error is 10.547 sec. The final RMSE for data without error is 0.0051742671 and for data with maximum 5% absolute relative random error is 0.019615273. Once again, one can see that for both cases they do not meet the convergence criterion for RMSE. However, after the process terminates the results are still acceptable.

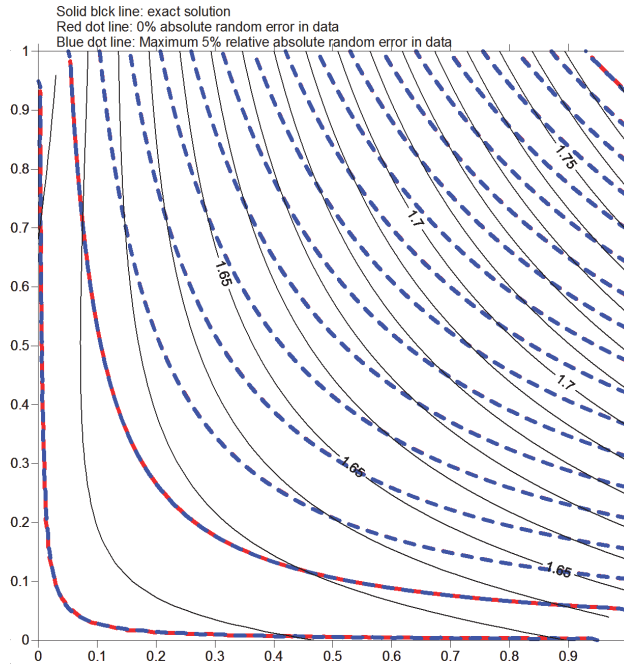


Figure 11: The temperature distribution for example 3.

### 3.4 Example 4

In this example, the physical problem in example 1 is redone again. The only difference is that instead of using Neumann data as one of the Cauchy data we replace the Neumann data by the nonlinear boundary condition in equation (6). All setup and parameters are the same as that in example 1. In this example, we only use Cauchy data with maximum 5% absolute relative random error. Since nonlinear boundary condition is used, the parameters used in equation (6) are:  $h=10$ ,  $\sigma = 5.667 \times 10^{-8}$ ,  $T_f = 1$ ,  $T_s = 1$  and  $\bar{\epsilon} = 1$ .

The result is sketched in figure 12. Compare this with figure 5, one can find out that using conventional Cauchy data seems better than using nonlinear Cauchy data (eq.(4) and eq.(6)) under the same noise level. The reason should come from the nonlinearity which may enlarge the errors in data during calculation.

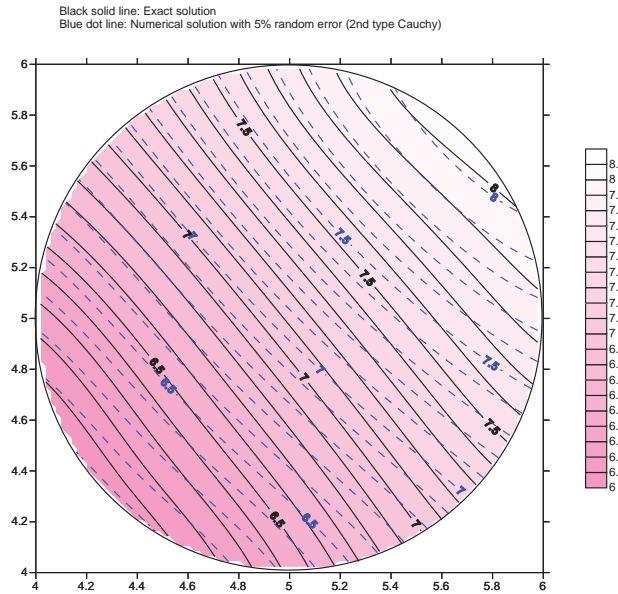


Figure 12: The temperature distribution for using Dirichlet and nonlinear Robin conditions as Cauchy data.

### 3.5 Example 5

In this example, a peanut shape domain is considered. The boundary curve is written as:  $\bar{r}(\bar{\theta}) = 0.3\sqrt{\cos 2\bar{\theta} + \sqrt{1.1 - \sin^2 2\bar{\theta}}}$   $0 \leq \bar{\theta} \leq 2\pi$  where  $(\bar{r}, \bar{\theta})$  are the cylindrical coordinate components. Total 100 equally distance points are placed on the boundary and 50 of them the Cauchy data are prescribed while for others no information is prescribed. The temperature dependent thermal conductivity is  $k(T) = \frac{1}{T}$  and the exact solution is designed as  $T(x, y) = \exp(xy + 2)$ . The Cauchy data are given on the upper half boundary, i.e.,  $0 \leq \bar{\theta} \leq \pi$ . For the remaining part of boundary, no information is given. Both 0% random errors and maximum 3% absolute relative random errors are added in Cauchy data. Totally 101 uniformly distributed interior points accompanied with boundary points are used to be source points. After the weights are obtained, 233 uniformly distributed interior points

and 100 boundary points are used to yield the temperature distribution. The setup for source points is illustrated in figure 13.

The value of  $a_c$  is 3.5, the value of  $\bar{\alpha}$  is 0.001, the converge criterion  $\varepsilon=0.05$  and the maximum iteration steps for the inner loop  $I_{max}=80,000$ . The initial guesses for the unknown weights of the radial basis functions are all 0.01.

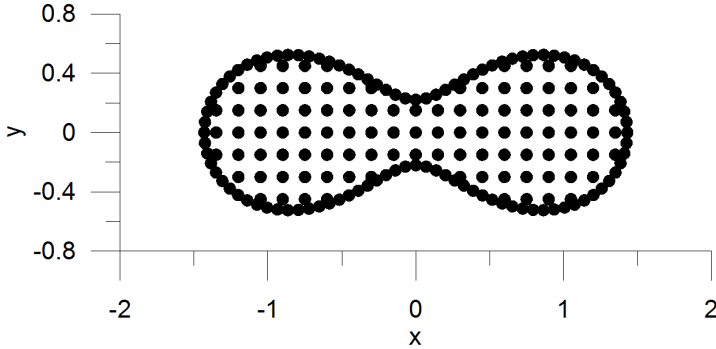


Figure 13: Source point setup for example 5.

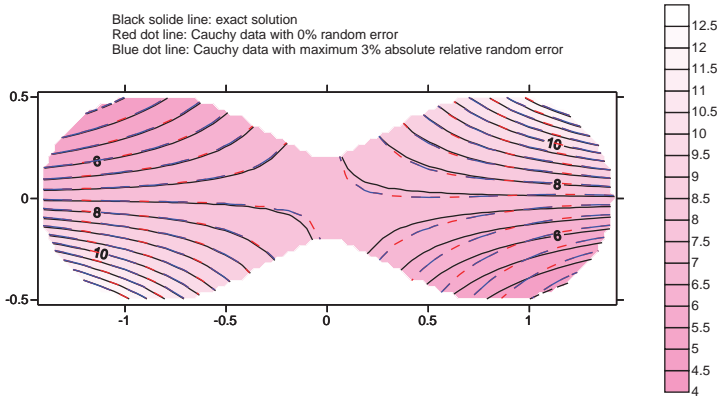


Figure 14: The temperature distributions for example 5.

The numerical results are shown in figure 14. It can be seen that the numerical results match the exact solution very well. The maximum absolute relative error percentage is less than 7 percent.

In this example, the DIP terminates due to the convergence criterion  $\varepsilon=0.05$  has been achieved for both cases with 0% and 5% maximum absolute relative random error in Cauchy data.

3.6 Example 6

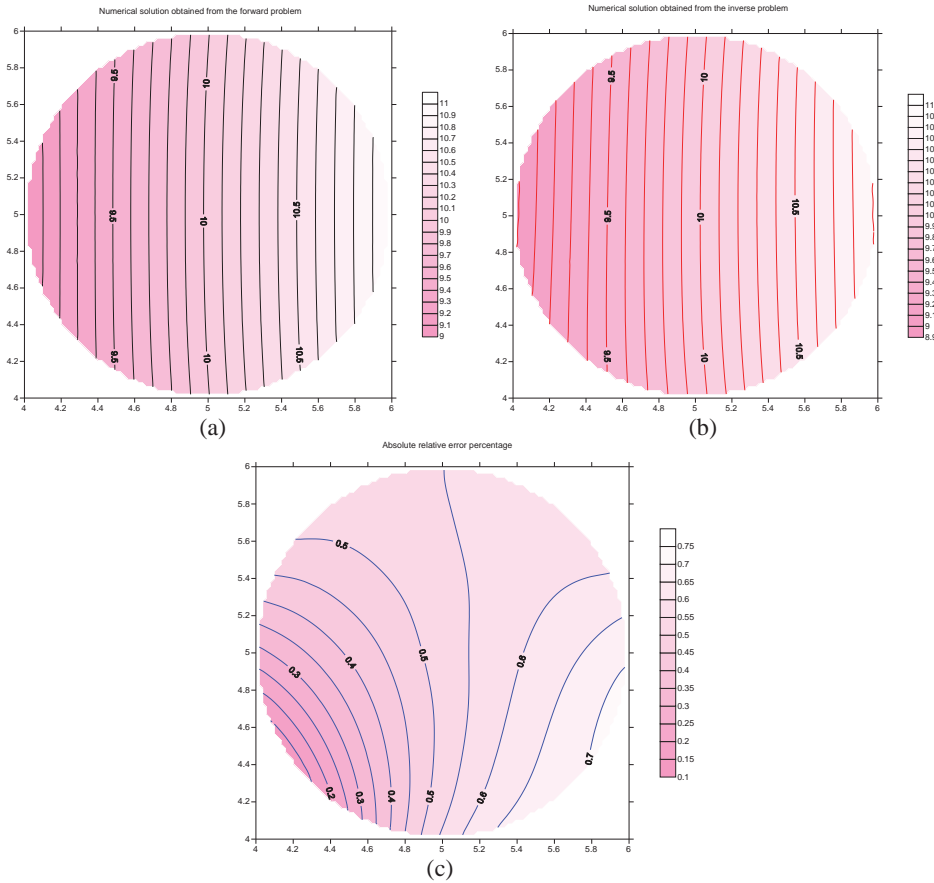


Figure 15: Numerical results: (a) Numerical solution for the forward problem; (b) numerical solution for the inverse Cauchy problem; (c) the absolute relative error percentage contour.

In the above five numerical examples, the numerical solutions are compared with analytical solutions. In real engineering problems, the so-called analytical solution may not exist. Therefore, the performance of DIP for inverse Cauchy problems without the analytical solution is quite interesting. In this example, the domain is a circular domain with radius equal to 1. The center of this circular domain is at (5,5). The parameters used are:  $\bar{\alpha} = 0.0001$ ,  $a_c = 2.0$ ,  $I_{max}=30000$ ,  $\epsilon=0.0001$ . The weights for the radial basis functions are set as 0.01 initially. The setup for boundary points, interior points and representation points are the same as that in

example 1.

The forward problem is first studied. The Dirichlet data is given as:  $T(\bar{\theta}) = 10 + \cos \bar{\theta}$  on the boundary where  $\bar{\theta}$  is the angle for the cylindrical coordinate system measuring from the center of the circular domain. The numerical solution for the forward problem is given in figure 15(a).

Then the Cauchy data made from the previous forward problem are used for the inverse Cauchy problem. The Cauchy data are prescribed for the upper half circle, i.e., for  $0 \leq \bar{\theta} \leq \pi$ . A maximum 5% absolute relative random error is added in Cauchy data. The remaining part of the boundary has no information. The results for this inverse Cauchy problem is illustrated in figure 15 (b). Comparing this with the numerical result obtained from the forward problem, one can find that the proposed DIP can deal with a problem without the analytical solution. The absolute relative error percentage is defined as:  $\kappa := \frac{\|T_{inverse} - T_{forward}\|}{\|T_{forward}\|} \times 100\%$ , and the contour for the absolute relative error percentage is shown in figure 15(c). One can find that the difference between the solution of the inverse Cauchy problem and that of the forward problem is very small.

#### 4 Conclusions

In this study, the double iteration process is used to deal with the Cauchy inverse problem of a nonlinear heat conduction equation. The double iteration process seeks for the appropriate evolution direction by using the MTRM for the inner loop. In order to avoid consuming too much computation time, once the direction satisfy the criterion  $a_0 < a_c$  or the steps for inner loop is greater than  $I_{max}$  the inner loop terminates. Once the RMSE is less than the prescribed value or the inner loop terminates because that the steps for inner loop is greater than  $I_{max}$ , the whole process is stopped. This double iteration process can theoretically find the most appropriate direction for each evolution step as well as avoid consuming too much CPU time. Six numerical examples are given to show the validity for this approach. Numerical results show that this approach is very efficient and can obtain accurate enough results for a nonlinear ill-posed inverse problem like the problem considered in this paper.

#### References

- Bialecki, R.; Nowak, A. J.;** (1981): Boundary value problems in heat conduction with nonlinear material and boundary conditions. *Appl. Math. Modelling*, vol. 5, pp.416-21.
- Cannon, J. R.** (1967): Determination of the unknown coefficient  $k(u)$  in the equa-

tion  $\nabla k(u)\nabla u = 0$  from overspecified boundary data. *Math. Anal. Appl.*, vol. 18, pp.112-14.

**Chan, H. F.; Fan, C. M.** (2013): The modified collocation Trefftz method and exponentially convergent scalar homotopy algorithm for the inverse boundary determination problem for the biharmonic equation. *Journal of Mechanics*, vol. 29, pp. 363-372.

**Chan, H. F.; Fan, C. M.; Yeih, W.** (2011): Solution of inverse boundary optimization problem by Trefftz method and exponentially convergent scalar homotopy algorithm. *CMC: Computers, Materials, & Continua*, vol. 24, pp. 125-142.

**Gesele, G.; Linsmeier, J.; Drach, V.; Fricke, J.; Arens-Fischer, R.** (1997): Temperature-dependent thermal conductivity of porous silicon. *Journal of Physics D: Applied Physics*, vol. 30, no.21, p. 2911.

**Hansen, P. C.** (1992): Analysis of discrete ill-posed problems by means of the L-curve. *SIAM Rev.*, vol. 34, pp. 561-580.

**Hardy, R. L.** (1990): Theory and applications of the multiquadric-biharmonic method. *Computers and Mathematics with Applications*, vol. 19, no.8/9, pp.163–208,.

**Hone, J.; Whitney, M.; Piskoti, C.; Zettl, A.** (1999): Thermal conductivity of single-walled carbon nanotubes. *Physical Review B*, vol. 59, no.4, pp.2514-2516.

**Ingham, D. B.; Yuan, Y.** (1993): The solution of a nonlinear inverse problem in heat transfer. *IMA Journal of Applied Mathematics*, vol. 50, pp.113-132.

**Ku, C.-Y.; Yeih, W.** (2012): Dynamical Newton-like methods with adaptive step-size for solving nonlinear algebraic equations. *CMC: Computers, Materials, & Continua*, vol. 31, pp. 173-200.

**Ku, C.-Y.; Yeih, W.; Liu, C.-S.** (2011): Dynamical Newton-like methods for solving ill-conditioned systems of nonlinear equations with applications to boundary value problems. *CMES: Computer Modeling in Engineering & Sciences*, vol.76, pp. 83-108.

**Landweber, L.** (1951): An iteration formula for Fredholm integral equations of the first kind. *Amer. J. Math.*, vol. 73, pp. 615–624.

**Liu, C.-S.** (2013): An Optimal Preconditioner with an Alternate Relaxation Parameter Used to Solve Ill-posed Linear Problems. *CMES: Computer Modeling in Engineering & Sciences*, vol. 92, pp. 241-269.

**Liu, C.-S.** (2012): Optimally generalized regularization methods for solving linear inverse problems. *CMC: Computers, Materials, & Continua*, vol. 29, pp. 103-127.

**Liu, C.-S.; Atluri, S. N.** (2008): A novel time integration method for solving a large system of non-linear algebraic equations. *CMES: Computer Modeling in*

*Engineering & Sciences*, vol. 31, pp. 71-83.

**Liu, C.-S.; Atluri, S. N.** (2011a): An iterative algorithm for solving a system of nonlinear algebraic equations,  $F(x)=0$ , using the system of ODEs with an optimum in  $\dot{\mathbf{x}} = \lambda [\alpha \mathbf{F} + (1 - \alpha) \mathbf{B}^T \mathbf{F}]$ ;  $B_{ij} = \partial F_i / \partial x_j$ . *CMES: Computer Modeling in Engineering & Sciences*, vol. 73, pp. 395-431.

**Liu, C.-S.; Atluri, S. N.** (2011b): Simple "residual-norm" based algorithms, for the solution of a large system of non-linear algebraic equations, which converge faster than the Newton's method. *CMES: Computer Modeling in Engineering & Sciences*, vol. 71, pp. 279-304.

**Liu, C.-S.; Atluri, S. N.** (2012): An iterative method using an optimal descent vector, for solving an ill-conditioned system  $\mathbf{B}\mathbf{X}=\mathbf{b}$ , better and faster than the conjugate gradient method. *CMES: Computer Modeling in Engineering & Sciences*, vol. 80, pp. 275-298.

**Liu, C.-S.; Kuo, C.-L.** (2011): A dynamic Tikhonov regularization method for solving nonlinear ill-posed problems. *CMES: Computer Modeling in Engineering & Sciences*, vol. 76, No.2, pp.109-132.

**Mintsu, H. A.; Roy, G.; Nguyen, C. T.; Doucet, D.** (2009): New temperature dependent thermal conductivity data for water-based nanofluids. *International Journal of Thermal Sciences*, vol. 48, no. 2, pp. 367-371.

**Morozov, V. A.** (1966): On regularization of ill-posed problems and selection of regularization parameter. *J. Comp. Math. Phys.*, vol. 6, pp. 170-175.

**Morozov, V. A.** (1984): *Methods for Solving Incorrectly Posed Problems*. Springer, New York.

**Tikhonov, A. N.; Arsenin, V. Y.** (1977): *Solution of Ill-posed Problems*. Washington: Winston & Sons.

**Tjalling, J. Y.** (1955): Historical development of the Newton-Raphson method. *SIAM Review*, vol. 37, pp. 531-551.

**Yeih, W.; Ku, C.-Y.; Liu, C.-S.; Chan, I.-Y.** (2013): A scalar homotopy method with optimal hybrid search directions for solving nonlinear algebraic equations. *CMES: Computer Modeling in Engineering & Sciences*, vol. 90, pp. 255-282.

**Yeih, W.; Chan, I.-Y. ; Ku, C.-Y.; Fan, C.-M.; Guan, P.-C** (2014): A double iteration process for solving the nonlinear algebraic equations, especially for ill-posed nonlinear algebraic equations. *CMES: Computer Modeling in Engineering & Sciences*, vol. 99, no. 2, pp. 123-149.